crystals

MDPI

Article

Antimicrobial, Antiasthmatic and Cytotoxic Activities of Silver Nanoparticles Synthesized by Green Method Using *Zingiber officinale* Extract

Murad A. Mubaraki [1], Kashif Mustafa [2], Fozia Fozia [3,*], Madeeha Aslam [2], Ijaz Ahmad [2,*] and Nisar Ahmad [4]

[1] Clinical Laboratory Sciences Department, College of Applied Medical Sciences, King Saud University, Riyadh 11433, Saudi Arabia
[2] Department of Chemistry, Kohat University of Science & Technology, Kohat 26000, Pakistan
[3] Biochemistry Department, Khyber Medical University Institute of Medical Sciences, Kohat 26000, Pakistan
[4] Department of Botany, Kohat University of Science & Technology, Kohat 26000, Pakistan
* Correspondence: drfoziazeb@yahoo.com (F.F.); drijaz_chem@yahoo.com (I.A.)

Abstract: In this study, effective and environmentally friendly methods were used to achieve the synthesis of silver nanoparticles (Ag NPs) by an aqueous plant extract. The Ag NPs were synthesized via *Zingiber officinale* plant extract that acted as a reducing and stabilizing agent. Various techniques, including UV-Visible spectroscopy (UV-Vis), X-ray diffraction pattern (XRD), Fourier transform infrared spectroscopy (FT-IR), and scanning electron microscopy (SEM) were used. The plant extract treated with silver nitrate solution at room temperature (27 ± 20) resulted in the successful synthesis of the Ag NPs, that were confirmed by UV-Vis spectroscopy. The crystalline morphology and size of the nanoparticles were calculated using Scherrer equation, that specify a face-centered cubic (fcc) crystalline structure with size ranges as 16 nm. The spherical geometry of Ag NPs was confirmed from scanning electron microscopy. FT-IR study validates the existence of several functional groups of active biomolecules such as -OH, C-O, C=C, C-O-C, and N-H that act as a reducing and capping agent for the synthesis of Ag NPs and were found in the extract. The synthesized Ag NPs were used to evaluated antimicrobial activity against different bacterial and fungal strains. The *Zingiber officinale*-Ag NPs exhibited maximum zone of inhibition against *Staphylococcus aureus* bacterial strain which were 17.8 ± 0.03 mm, and *Fusarium graminium* fungal strain showed 11.0 ± 0.01 mm at 80 µg/mL concentrations, *respectively*. Furthermore, the Ag NPs were considered to be a significant anti-asthma agent that decreased the white blood cells (WBC), eosinophils (EOS) in blood level, and wet/dry (W/D) weight proportion of the lung at 24 µg/g/day. The cytotoxicity of synthesized nanoparticles shows that the concentration under 90 µg/mL were biologically compatible.

Keywords: green synthesis; *Zingiber officinale*; Ag NPs; antimicrobial; antiasthmatic; cytotoxic activities

Citation: Mubaraki, M.A.; Mustafa, K.; Fozia, F.; Aslam, M.; Ahmad, I.; Ahmad, N. Antimicrobial, Antiasthmatic and Cytotoxic Activities of Silver Nanoparticles Synthesized by Green Method Using *Zingiber officinale* Extract. *Crystals* **2023**, *13*, 333. https://doi.org/10.3390/cryst13020333

Academic Editors: Abdur Rauf and Mujeeb Ur Rehman

Received: 29 January 2023
Revised: 9 February 2023
Accepted: 13 February 2023
Published: 16 February 2023

1. Introduction

Metallic nanoparticles have a limited set of optical, thermal, chemical, and physical properties because they have a surface atom with a higher energy than bulk materials and an electron free path that is measured on a nanoscale ranges (10–100 nm) for metals nanoparticles at room temperature. It can be challenging in nanotechnology to regulate the size and shape of nanoparticle in order to modify their properties [1]. Metal oxide nanoparticles (MNPs) such Fe_3O_4, CuO, TiO_2, and ZnO, in particular their significant anti-inflammatory and antibacterial characteristics, have recently been the subject of extensive research for biological impacts [2]. Due to their distinctive properties in a variety of fields, including pharmaceuticals, home appliances, optical sensors, cosmetics, diagnostics, and orthopedics, Ag NPs have undergone extensive analysis among other metal nanoparticles. That has been improved the tumor-killing properties of anticancer medications through Ag NPs [3]. Nano-sized Ag NPs have been used as an antibacterial agent against both

anaerobic and aerobic microbes because of their remarkable surface to volume ratio. Ag NPs have a strong antibacterial effect because they generate free radicals on their surface, which can penetrate cell membranes and impair cellular functions [4]. Various physical and chemical methods, such as chemical reduction, solvo-thermal synthesis [5], plasma irradiation, [6] and laser ablation [7], were used for the synthesis of nanoparticles. These methods have inherent drawbacks, such as increased size, high energy requirements, quite expensive, time-consuming, energy-consuming, environmentally toxic, and capital intensiveness. Therefore, biological approaches for the synthesis of Ag NPs have been suggested as possible eco-friendly, low-cost, authentic, efficient, reproducible alternatives to chemical and physical methods. Since, some of the groups have been reported on the synthesis of Ag NPs utilizing various plant extracts, such as, *Andrographis paniculata* [8], *Cathranthus roseus* [9], and *Rhynchosia suaveolens* [10] that function as a reducing and stabilizing agent.

In order to synthesized Ag NPs, the current research was carried out by utilizing an aqueous extract of the *Zingiber officinale* plant, which is a member of the Zingiberacae family. It is one of the most popular spices in the world. In the Ayurvedic, Siddha, Chinese, Arabic, African, and Caribbean medical systems, it has been traditionally used to treat a number of ailments, such as nausea, vomiting, asthma, coughing, palpitations, inflammation, dyspepsia, loss of appetite, constipation, indigestion, and pain [11]. The therapeutic potential of *Zingiber officinale* has been recently investigated utilizing state-of-the-art scientific methods. A number of bioactive compounds have been extracted from the plant and have systematized for pharmacological challenges. The phytochemical composition of *Zingiber officinale* contains tannin, essential oils, phenolic compounds, flavonoids, carbohydrates, proteins, alkaloids, glycosides, saponins, steroids, terpenoids, and glycosides that act as a reducing and stabilizing agent for the synthesis of Ag NPs [12].

An inflammatory disorder of the airways known as bronchial asthma is caused by a complicated interplay between heredity and environmental variables. It is characterized by different airway obstruction, airway inflammation, and bronchial hyper reactivity. Approximately 7–10% of people worldwide have bronchial asthma. The most prevalent incapacitating sickness among the several respiratory illnesses that affect people, is bronchial asthma. Despite a vast variety of medications being readily available, the comfort they provide is primarily symptomatic and transient. Additionally, these medications have negative effects. Therefore, there is an urgent need for effective and safe bronchial asthma treatments [13]. Furthermore, the intensification of microorganism needs to resistance the growth of many antimicrobials, extensive topical drugs are uses as antibiotics. Due to the synergistic impact of combining the two resources, the intrinsic biological activity of plant extracts may be increased when combined with Ag NPs. Ideally, no antibiotic meant for systemic use (or related to an antibiotic for systemic use) should be applied topically, due to risks of promoting resistance to the systemic antibiotic. Ag NPs are an attractive alternative to topical medications due to their excellent antibacterial activity and capacity to decrease the threat of multidrug-resistant bacteria [14]. Different biological methods have been reported on the synthesis of Ag NPs and their potential antimicrobial activity. As a part of our continuous interest on green synthesis of Ag NPs [15], the current work is based on green synthesis of Ag NPs and explore their antimicrobial, antiasthmatic and cytotoxic activities. There has not been any specific research available on antimicrobial activity against selected pathogens and antiasthmatic activity of Ag NPs synthesized by *Zingiber officinale* aqueous extracts. Therefore, as a highly significant biological source for treating a wide range of diseases, this medicinal herb (*Zingiber officinale*) was selected and in this article, we are reporting it for the first time. Furthermore, the morphological, optical, and geometrical characteristics of the synthesized Ag NPs were examined by different techniques, including the X-ray diffractometer, scanning electron microscope (SEM), Fourier transform infrared spectroscopy (FT-IR), and UV-Visible spectrophotometry. Moreover, the current study evaluates in vitro antimicrobial, antiasthmatic activity and checks its biocompatibility for practical application by using cytotoxic activity.

2. Materials. and Methods

2.1. Preparation of Plant Extract

Zingiber officinale plant roots were attained from a local market of Kohat, KPK, Pakistan, and dried in a vacuum oven (JSOF-100H, JS Research Inc. 69, Gumsang-gogaegil, Gongju, Republic of Korea) after being washed multiple times with distilled water. These clean and dust-free roots were processed by using a blender to obtain a fine ground powder. The distilled water was used to prepare 5% solution. The mixture was heated on a hot plate while being agitated for 30 min. After that, it was filtered, and the filtrate was kept in a refrigerator at 4 °C for green synthesis of Ag NPs.

2.2. Green Synthesis of Ag NPs

The green synthesis of target Ag NPs was achieved by consuming 1 mM concentration of the prepared silver nitrate (Sigma-Aldrich, >98%, Darmstadt, Germany) solution in an aqueous medium. The ratio of 1:6 (v/v) was used by thoroughly mixing the solution of 1 mM silver nitrate with a solution of plant extract (5%) to synthesize Ag NPs. The plant extracts served as both capping and reducing agents. The Erlenmeyer flask containing 6 mL of plant extract was mixed into 1 mM $AgNO_3$ solution for the synthesis of Ag NPs, and at 70 °C temperature were applied to the reaction mixture and was continuously stirred in a rotatory orbital shaker for 24 h. The color of reaction mixture had changed from bright green to dark brown and then examined using an ultraviolet/visible spectrophotometer. The samples were then centrifuged to remove the solvent from the residue, which was then rinsed two to three times with distilled water. Powdered nanoparticles were obtained, which were employed for further characterizations and subsequent applications [16].

2.3. Characterization of Ag NPs

Various spectroscopic techniques were used to characterize and confirm the synthesis of Ag NPs.

2.3.1. UV-Vis Spectroscopy

UV-Visible spectroscopy (spectrophotometer, Perkin-Elmer Lamda 35, Waltham, MA, USA) was used to assess the optical characteristics of Ag NPs. Synthesis of Ag NPs by using an aqueous plant extract were characterized by UV-Visible spectroscopy that were recorded in wavelength ranges between 200 to 800 nm, up to 24 h time intervals. The synthesis of Ag NPs was confirmed by the reduction in Ag^+ to Ag^0.

2.3.2. FT-IR Analysis

FT-IR spectrometer was used to investigate the chemical composition of green synthesized Ag NPs (Bruker, Alpha-II, Billerica, MA, USA). The KBr pellets were used to characterize the solution containing Ag NPs that was centrifuged, vacuum dried and recorded within the range of 400–4000 cm^{-1}. The FT-IR spectrum of an aqueous extract was obtained by drying the plant extract at 25 °C in an oven. The spectra were recorded using attenuated total reflectance technique. Fourier transform infrared spectroscopic analysis (FT-IR) also known as functional group identification spectroscopy. The evaluation of the functional group of a plant extract that serves as a reducing agent and stabilizing agent, as well as the synthesis of Ag NPs. In this analysis, the extract and powder Ag NPs were used.

2.3.3. XRD Analysis

The powder X-rays diffraction spectroscopy technique (Brikar-D8 advance, Bruker, Billerica, MA, USA) was utilized by the characterization of particle size and phase purity of the synthesized Ag NPs. The X-ray CuKa source at 30 kV voltage, a current of 20 mA, and a scanning rate of 0.030/s were employed to investigate the synthesis of Ag NPs. To identify the crystallinity of metallic nanoparticles, the data of all the samples of X-ray diffraction were obtained at 2θ degree angle and ranging from 20 to 80°.

2.3.4. SEM Analysis

The Scanning Electron Microscope (SIGMA HV-Carl Zeiss, Oberkochen, Germany) was utilized to the morphological characterization of the green synthesized Ag NPs using *Zingiber officinale* plant extracts. Smears of the nanoparticle solution were applied to the slides to prepare the SEM slide. The simples were characterized using SEM at a 20 kV accelerating voltage.

2.4. Antimicrobial Evaluations

2.4.1. Mueller Hinton Agar (MHA) Medium

The Mueller Hinton Agar (MHA) medium was used to evaluate the antimicrobial potential of the synthesized nanoparticles. The ingredients beef Extract 2 g/L, acid hydrolysate of casein 17 g/L (Sigma-Aldrich, >98%, Germany), peptone 10 g/L (Biotecnica International S.A. de C.V., Oax. Oaxaca, Mexico), starch 1.5 g/L, and agar 17 g/L were used to prepare Mueller Hinton Agar (MHA) medium. The pH of the medium was eventually stabilized at (7.3) and temperature of 25 °C.

2.4.2. Antimicrobial Assay

The antibacterial activity of the green synthesized Ag NPs were evaluated using the agar well diffusion type of technique [17]. Four bacterial strains used in the studies are *Staphylococcus Aureus, Pseudomonas aeruginose, Klebsiella Pneumoniae, and Salmonella typhi.* The three fungal strains *Fusarium graminium*, *Alterneria alternative*, *and Candida albicane* were used to evaluate the biocidal potential of synthesized nanoparticles against pathogenic diseases. All these organisms were taken from Department of Microbiology Kohat University of Science & Technology, Kohat, Pakistan. In order to ensure the MHA medium, 11.4 g of MHA was evenly distributed in 300 mL of distilled water followed by constantly heated. The mixture was autoclaved at 10 lbs. of pressure at 115 °C temperature for 30 min. Approximately 20 mL mixtures were transferred into sterilized petri dishes in the laminar flow hood. The petri plate was kept for solidification purposes for 15 to 20 min. To check further contamination all these plates were left at room temperature for overnight. Next, an agar well measured 6 mm in diameter and 2.5 mm in depth was used to bored on the exterior of the medium by using a fine stainless steel cork hole [18]. Each plate was marked and filled with different concentrations of the synthesized Ag NPs (20 µg/mL, 40 µg/mL, 60 µg/mL and 80 µg/mL), whereas standard drugs were employed as a positive control. The samples were introduced into nutrient agar prior solution and then followed by adding bacterial and fungal strains from one-day old culture, respectively. The culture containing synthesized Ag NPs was sealed with parafilm and incubated for 24 h at 37 °C temperature. Amoxicillin and fluconazole (0.5 to 15.00 µg/mL) were used as positive controls for bacteria and fungus, respectively, while dimethyl sulfoxide (DMSO) served as a negative control. After the completion of the growth period, the plates were checked for zone inhibition. A screw gauge was used to measure the diameter of the zone of inhibition. The results were tabulated and the values for each organism were expressed in millimeter (mm), each experiment repeated out in triplicates. After that the percent (%) zone of inhibition was measured, which were compared with the standard.

2.5. Antiasthma Assays

2.5.1. Asthmatic Model Preparation and Drug Treatment

The antiasthma activity of Ag NPs was examined Wistar rats which were accumulated from the Neuro Molecular Medicine Research Center (NMMRC), Peshawar, Khyber Pakhtunkhwa, Pakistan). In order to evaluate the anti-asthmatic activity, the OVA-induced model was applied. In this experiment, the animals were sensitized within the peritoneal cavity through OVA (100 mg/mL) in 0.9% PBS saline for different time intervals (0, 7, and 14 days). The solution was diluted to 1 mL of Al $(OH)_3$ adjuvant, because Al $(OH)_3$ is the most common adjuvant in human vaccines that enhanced the immune responses against antigens contained in the vaccine. After 14 days, the rats were breath 2% of OVA or

saline for 30 min. The Wistar rats were divided into six groups, each group contains 5 rats, (n = 30) including the control, dexamethasone, plant extract, and Ag NPs. Different concentrations of plant extract and Ag NPs (6, 12, and 24 µg/g/day) were used to investigate the anti-asthmatic activity. In this, the PBS treated group was used as a negative control and dexamethasone-treated group (0.75 g/kg) used as a positive control [19].

2.5.2. Measurement of Latent Period

Latent period is the time that passes between the exposure to something (such as radiation or a virus) that can cause disease and having symptoms. The signs of the latent period, such as itching, wheezing, nodding respiratory, and cough, were measured within 5 min of the last exposure to OVA aerosol [20].

2.5.3. White Blood Cell and Eosinophils Analysis

After 24 h of the last exposure to OVA aerosol, the rats were desensitized by peritoneal cavity with chloral hydrate (7%). A heparin-coated tube was used to collect the anticoagulated blood by inserting cannula to the abdominal aorta. An YZ-Hemavet Analyzer was used to count the number of eosinophils (EOS) and white blood cells (WBC) in the blood [21,22].

2.5.4. Measurement of Wet and Dry Weight of Lungs

A variation in the wet to dry weight ratio (W/D) of the lungs caused damage to the lungs of unaffected rodents. The wet/dry weight analysis was used to determine the amount of water present in the lung sample. The right lung was separated and weighted. A constant dry weight was achieved by folding the tissue sample in aluminum foil and drying it, at the 100 °C temperature for 4–5 days before weighing it once again (dry weight) [23].

2.6. Cytotoxic Activity of Ag NPs

MTT Assay

In this study, the cytotoxic effects of the synthesized Ag NPs were investigated by utilizing the HepG2 cell line (hepatocellular carcinoma cell line). HepG2 cells were cultured in supplemented DMEM by mixing 100 µg/mL of streptomycin, 10% FBS, and penicillin (100 µg/mL). The cells were kept in a 5% CO_2 atmosphere at 37 °C temperature. By using the MTT assay, the viability activity of the green synthesized Ag NPs was tested against the HepG2 cell [24]. In a 96-well plate an equivalent amount of HepG2 cells (about 6×10^3 cells) was grown, and the cells were subsequently treated with synthesized Ag NPs at various concentrations. Each well received 50 µL of the reconstituted MTT solution (2 mg/mL) after 48 h of incubation. Cells were grown without Ag NPs as a control group. The plate was then gently shaken for 4 h at 5% CO_2 and 37 °C during incubation. After that, purple color formazan crystals formed, that were dissolved in 150 µL of dimethyl sulfoxide (DMSO). The optical density of the solution was measured by microplate reader (Genetix580, Biotech Asia Pvt. Ltd., Shivaji Marj, India) at 570 nm.

2.7. Ethical Statement

Ethical approval of the study was obtained from the ethical committee of Neuro Molecular Medicine Research Center (NMMRC), Peshawar, Khyber Pakhtunkhwa, Pakistan under the reference No. NMMRC-KM-3042 dated 20 April 2021.

2.8. Statistical Analysis

All the experiments were carried out in triplicate, and the statistical analysis was carried out using SPSS (version 25, SPSS Inc., Chicago, IL, USA). The results were summarized as arithmetic mean ± standard deviation. The analysis of variance was used to determine statistical significance, followed by control group with experimental group.

3. Results and Discussion

3.1. UV-Visible Analysis of Ag NPs

The present investigation used *Zingiber officinale* aqueous plant extract because it contains phyto constituents that act as a bioactive green reducing agent, that transform Ag^+ into Ag NPs. It was possible to identify the green synthesis of Ag NPs (plant extract solution) by changing the color of the solution from yellow to a reddish-brown color, confirming the synthesis of Ag NPs. After that the reaction mixture was observed under UV-Vis spectroscopy. It was examined that the absence of an absorbance peak in the visible region when the samples were assessed in a UV-visible spectrophotometer, as showed in Figure 1A. However, the synthesis of Ag NPs was achieved by mixing Ag NO_3 solution with the plant extract at a volume of 1:6 (v/v). Therefore, the peak at wavelength of 444 nm was used to evaluate the synthesis of Ag NPs, that signifies surface plasmon resonance (SPR) carried on by the excitation of free electrons in metal [25,26]. The optical characteristics of the silver nitrate solution were changed as a result Ag^+ reduce to elemental Ag^0 and subsequent formation of Ag NPs were formed when it exposed to the bioactive components of plant extract [27].

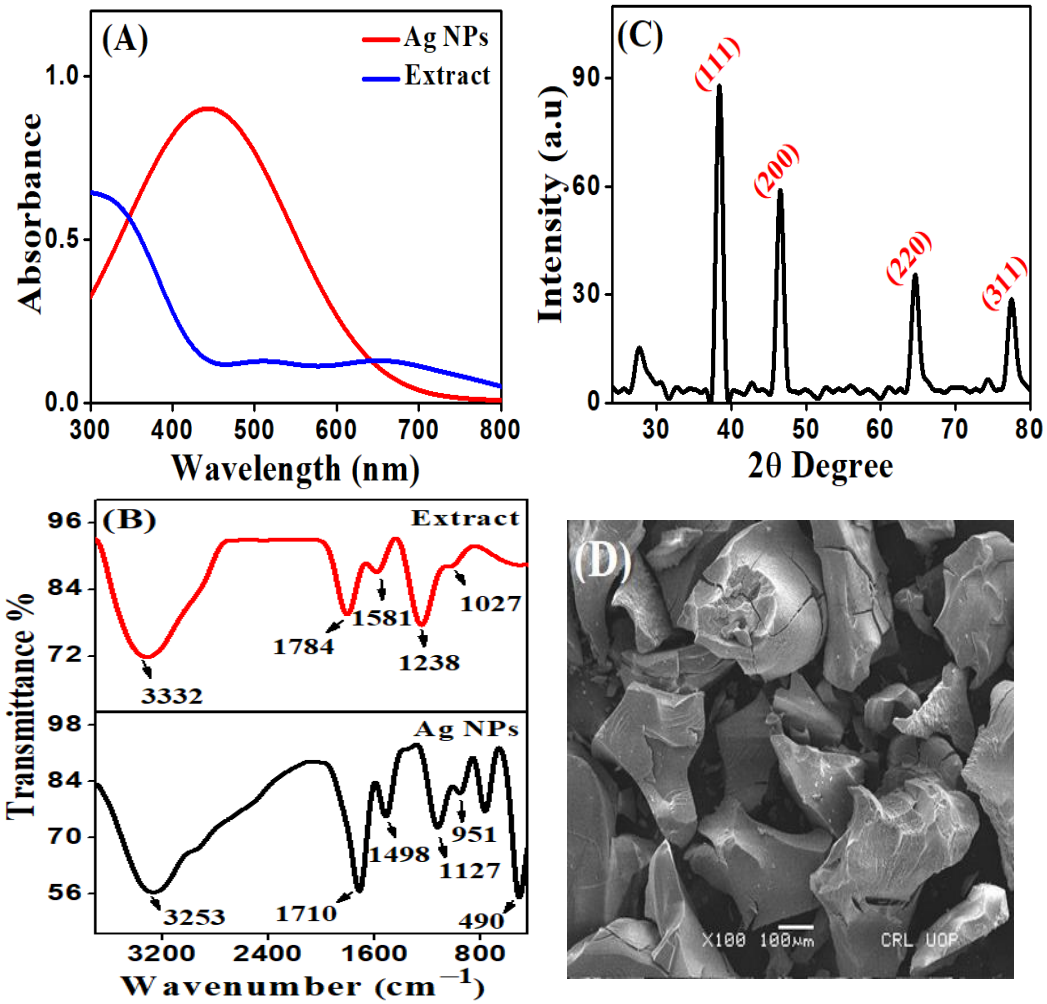

Figure 1. UV-visible spectroscopy of Ag NPs and *Zingiber officinale* plant extract (**A**), FT-IR spectra of synthesized Ag NPs and an aqueous plant extract of *Zingiber officinale* (**B**), XRD of Ag NPs synthesized by *Zingiber officinale* plant Extract (**C**), SEM image of Ag NPs under 100 µm (**D**).

3.2. FT-IR Analysis of Ag NPs

The FT-IR spectroscopy was used to analyze the biomolecules present in an aqueous plant extract of the Zingiber officinale that reduces Ag^+ to Ag^0. The functional groups

involved in the synthesis of silver nanoparticles are revealed by analyzing the FT-IR spectra of the *Zingiber officinale* plant extract and Ag NPs. In FT-IR spectra of the plant extract showed various absorption bands at 1027, 1238, and 1581 cm^{-1} that were caused by C-N stretching of amide I bond of proteins arising from carbonyl stretching in proteins, C-O-C groups of polyols such as flavones and polysaccharides, and C=C stretching of the methylene groups, respectively [28]. The sharp band at 1784 cm^{-1} were risen by the stretching vibration of C=O present in carbonyl functional groups, as shoed in Figure 1B. The significant band at 3332 cm^{-1} were corresponds to the stretching vibration of -OH functional groups found in alcohols and polyphenolic groups [29,30] Whereas, the FT-IR spectra of Ag NPs showed a considerable change in the absorption peaks at 951, 1127, 1498, 1710, and 3253 cm^{-1}, respectively. The change in absorption band indicating the functional groups interacted with the surface of the Ag NPs after the addition of $AgNO_3$ solution to the aqueous plant extract. However, the new band appears at 490 cm^{-1} specify M-O bond, due to oxidation-reduction potential of biomolecule such as polyphenol and its derivatives was used to reduce silver ions into silver nanoparticles [31]. Recently, *plant Zingiber* officinale contains different biomolecules such as flavonoids, carbohydrates, proteins, alkaloids, glycosides, saponins, steroids, and terpenoids, these biomolecules are helpful in the bioreduction of Ag^+ to stability Ag NPs [12,32]. It is still unclear how a silver ion is bio-reduced by phytochemical substances found in plant extracts. However, green synthesis involves the reduction in silver ions, that act as stabilizing and capping agent. According to the literature, the phytochemicals including polyphenols, proteins, glycosides, alkaloids and terpenoid that contain a high density of -OH groups [12]. Hydroxyl group of the polyphenols oxidizes and releases electrons [33]. These electrons are responsible for the reduction in Ag+ [34]. After the Ag^0 formation, many reactions need to occur in the Ag NPs formation, since atomic Ag^0 is not considered as a nanoparticle, its agglomeration forms nanoparticles by nucleation reactions. Complexation of polyphenol with silver ions, and the bond formed with the biomolecules is responsible for the stabilization of the nanoparticles [35].

3.3. XRD Pattern of Ag NPs

The X-ray diffraction pattern showed the crystallinity of Ag NPs synthesized from an aqueous plant extract Figure 1C. The X-ray diffraction (XRD) pattern was conducted 20–70 at 2θ degree, as mentioned in Figure 1C. The diffraction peaks with 2θ degrees at 38.1°, 44.3°, 64.4°, and 77.4° can be indexed to the (111), (200), (220), and (311) Bragg's reflections of the face-centered cubic (fcc) crystalline structure of Ag NPs, respectively. This diffraction pattern was very similar to JCPDS file no. 87-0720 standard diffraction pattern [36]. The following Debye-Scherrer formula was used to calculate the average particle size of Ag NPs.

$$D = 0.9\,\lambda/\beta\,\cos\theta, \quad (1)$$

where is the D was the regular crystalline size, lambda (λ) was the x-ray of the wavelength (nm), beta (β) corresponds to the angular line with at half maximum intensity as radian and θ represent the Braggs angle. The calculated particle size was the 16 nm for the face centered cubic Ag NPs synthesized from *Zingiber officinale* plant extract.

3.4. SEM Analysis of Ag NPs

The geometrical and morphological features of Ag NPs were assessed by using the SEM analysis [37]. The results demonstrate that Ag NPs were irregular morphology and size ranges 20–80 nm. The SEM images in Figure 1D revealed that Ag NPs were gathered throughout the surface of the sample. Ag NPs are synchronized in the form of large clusters, the aggregation of Ag NPs was observed in SEM images, which could be due to the evaporation and removal of solvent used during sample preparation. Solvent removal causes electrostatic forces to bring Ag NPs closer together and aggregated. Therefore, it appears to be greater-sized, but some of them are distributed, and a random spherical shape was confirmed from the given images using the ImageJ software (version 1.46) [38].

3.5. Antimicrobial Activity

3.5.1. Antibacterial Potential of the Synthesized Ag NPs

To explore the antibacterial. activity of the synthesized nanocrystal of silver nanoparticles against four different bacterial strains were selected. These bacterial strains are pathogenic to human and cause different diseases. Therefore, we select these bacterial strains under the area of examination at different concentrations. The agar well diffusion way was used to study the antimicrobial activity of the synthesized Ag NPs. The examined bacteria were *Staphylococcus Aureus, Pseudomonas aeruginose, Klebsiella Pneumoniae, and Salmonella typhi*. The Ag NPs showed potent antibacterial effect at all concentrations against all of the investigated microorganisms. It was observed that Ag NPs showed highest activity 17.8 ± 0.03 mm against *Staphylococcus Aureus,* whereas others showed 15.1 ± 0.04 mm, 15.0 ± 0.04 mm, 14.4 ± 0.05 mm against *Pseudomonas aeruginose, Klebsiella Pneumoniae, and Salmonella typhi* at 80 µg/mL, respectively. Amoxicillin was used as a standard. Table 1 enlists the antibacterial results of Ag NPs, which confirmed that the synthesized nanoparticles were active against various bacterial strains. The results showed that maximum zone of inhibition was observed by increasing the concentration of Ag NPs. Up to certain limit the synthesized nanoparticles showed promising results, but none of the nanoparticles, showed high inhibition zone than the standard antibiotic [39,40]. Sakthi Periasamy et al. used different microorganisms at different concentrations of Ag NPs such as 5 µg/mL, 10 µg/mL, 15 µg/mL, 20 µg/mL, and 40 µg/Ml. Ag NPs were used to check the antimicrobial activity against different bacterial strains including, *E. coli*, *P. aeruginosa*, *S. aureus*, and *B. subtilis*. It was found that *S. aureus* had a strong resistance to the Ag NPs in different concentrations [41]. D. Nayak et al. also investigated the antimicrobial activity of Ag NPs synthesized by using Hibiscus flower and used against the *Escherichia coli*, *Staphylococcus aureus*, *Vibrio cholerae*, and *Klebsiella pneumoniae,* that evaluate maximum zone of inhibition at concentrations of 100 µg/mL. Similar to the above results, the Ag NPs in the present study proved to be an active in a dose-dependently manner agent against different pathogens [42].

Table 1. Concentration of zone of inhibition.

Concentration (Zone of Inhibition in mm) Ag/*Zingiber Officinale*-NPs.					
Bacterial Strains	**20 µg/mL**	**40 µg/mL**	**60 µg/mL**	**80 µg/mL**	**Standard**
Staphylococcus Aureus	13.5 ± 0.03	15.6 ± 0.01	16 ± 0.03	17.8 ± 0.03	21.8 ± 0.07
Pseudomonas aeruginose	12.7 ± 0.05	14.3 ± 0.04	15.0 ± 0.05	15.1 ± 0.04	20 ± 0.04
Klebsiella Pneumoniae	9.8 ± 0.02	12.5 ± 0.03	14.9 ± 0.06	15.0 ± 0.04	22.5 ± 0.05
Salmonella typhi	12.6 ± 0.03	11.8 ± 0.06	15.8 ± 0.07	14.4 ± 0.05	21.8 ± 0.04
Fungal Strains					
Fusarium graminium,	9.0 ± 0.03	9.5 ± 0.01	10.5 ± 0.01	11.1 ± 0.01	12.8 ± 0.01
Alterneria alternate	10.2 ± 0.05	10.5 ± 0.04	10.7 ± 0.04	10.8 ± 0.04	12.0 ± 0.04
Candida albicane.	9.8 ± 0.02	10.2 ± 0.03	10.0 ± 0.03	10.3 ± 0.03	13.1 ± 0.03

Amoxicillin as a positive control, DMSO as a negative control for bacterial strains. Fluconazole as a positive control, DMSO as a negative control for fungal strains.

3.5.2. Antifungal Activity of Synthesized Ag NPs

To investigate the antifungal activity of synthesized nanoparticles that act as biocide agents against a variety of fungal strains, including, *Fusarium graminium, Alterneria alternate, Candida albicane.* The agar dilution technique was used to examine the antifungal efficacy of the synthesized Ag NPs. The drugs fluconazole was used as a standard drug. The obtained tabular form data of Ag NPs against antifungal effects, as shown in Table 1. Among all the fungal strains, *Fusarium graminium* showed higher activity 11.1 ± 0.01 mm, whereas other fungal strains minimum inhibition 10.8 ± 0.04 mm, 10.3 ± 0.03 mm against *Alterneria*

alternate, Candida albicane at 80 µg/mL concentration. This is because, silver salt has a clear mechanistic approach that firmly bond itself Ag+ ion to the thiol group (-SH) of different protein and denature it, which confirmed that when microbe treated with silver-based nanoparticles its DNA replication diminished and so therefore causes microbial death. Additionally, silver nanoparticles cause alteration in cell layer and change the electron thick granules shapes by combination of silver to Sulphur [43]. Panacek et al. report earlier that when the concentrations of Ag NPs increased than it can significantly inhibit the growth of fungi [44]. *Similarly*, Pallavi S.S et al. displayed significant antifungal potential of selected pathogenic fungi against *C. albicans*, *A. alternata*, *C. glabrata* and *F. oxysporum*. The least antifungal activity was recorded against *C. albicans* followed by *F. oxysporum* and *C. glabrata* [45].

3.6. Antiasthma Activity of Ag NPs

The trachea and lungs are the two major components of the respiratory system, that are sensitive to environmental factors. Therefore, the anti-asthma activity of the Ag NPs was employed. The WBC and EOS levels of blood, and the W/D lungs weight ratio were dramatically decreased and OVA-induced latent period in the anti-asthma test were increases by increasing the concentration Ag NPs, and which was greatly affected by the yeast-induced fever reaction (Figure 2) [20,21]. The levels of EOS and WBC in the blood were suppressed by varying concentrations of the Ag NPs from 6, 12, and 24 µg/g/day. The findings demonstrate that the effects of synthesized Ag NPs more significant than those of dexamethasone at 24 µg/g/day concentrations, respectively. Similarly, Ag NPs was also administered to reduce the W/D weight ratio of lungs at same concentrations, it also showed greater efficacy than dexamethasone. The studies demonstrate that synthesized Ag NPs are efficient as an anti-asthmatic by decreasing EOS and WBC in the blood, the W/D weight ratio of the lungs, and prolonging the latent period. Furthermore, the plant extract-treated group did not show activity at lower concentrations, but when the concentrations increased to 24 µg/g/day they became an active against anti-asthmatic activity. In contrast, Ag NPs showed excellent activity at lower concentrations, that was due to the large surface area and size-dependent nano properties of Ag NPs which are helpful in drug delivery systems. A similar report was examined by Mei, Fen, et al. using *Ephedra-Gypsum* extracts at concentrations of (6, 12, 24 µg/kg) significantly and dose-dependently attenuated yeast-induced fever in rats. The *Ephedra-Gypsum* extracts also reduced OVA-induced increases in eosinophils and the WBC, and decreased the wet and dry weight ratio of the lungs in the anti-asthmatic test [20].

3.7. Cytotoxicity Activity of Ag NPs on HepG2 Cell Line

The cell viability study of nanoparticles was performed using the MTT reduction test to determine the biocompatibility of Ag NPs. HepG2 cells were cultured in a 96-well microplate for 48 h at 37 °C and 5% CO_2 after being treated in vitro with synthesized Ag NPs at different concentrations (10, 30, 50, 70, and 90 µg/mL). Figure 3 showed that synthesized Ag NPs had a concentration-dependent rate of cell survival. The fact that cell viability decreased alongside increasing the concentration of Ag NP concentration suggests that Ag NPs might accumulate inside of cells, increasing stress and ultimately causing cell death. Other investigations have discovered that Ag NPs have the same cytotoxic activity for a variety of cancer cells [46]. Clearly, the current results demonstrated the Ag NPs synthesized by an aqueous plant extract showed significant efficiency against various biological activities. Numerous studies have demonstrated that biologically active substances such as flavonoids and phenols, which were harmless for healthy cells but lethal to cancer cells [47]. As previously mentioned, the *Zingiber officianale* is a rich source of polyphenols and flavonoids, which is responsible for the antimicrobial activity [48]. Ag NPs cytotoxicity is most likely brought on by the silver ions that was favorable to the physical and chemical interactions with the functional groups of proteins in cells and the nitrogen or phosphate groups in DNA [49].

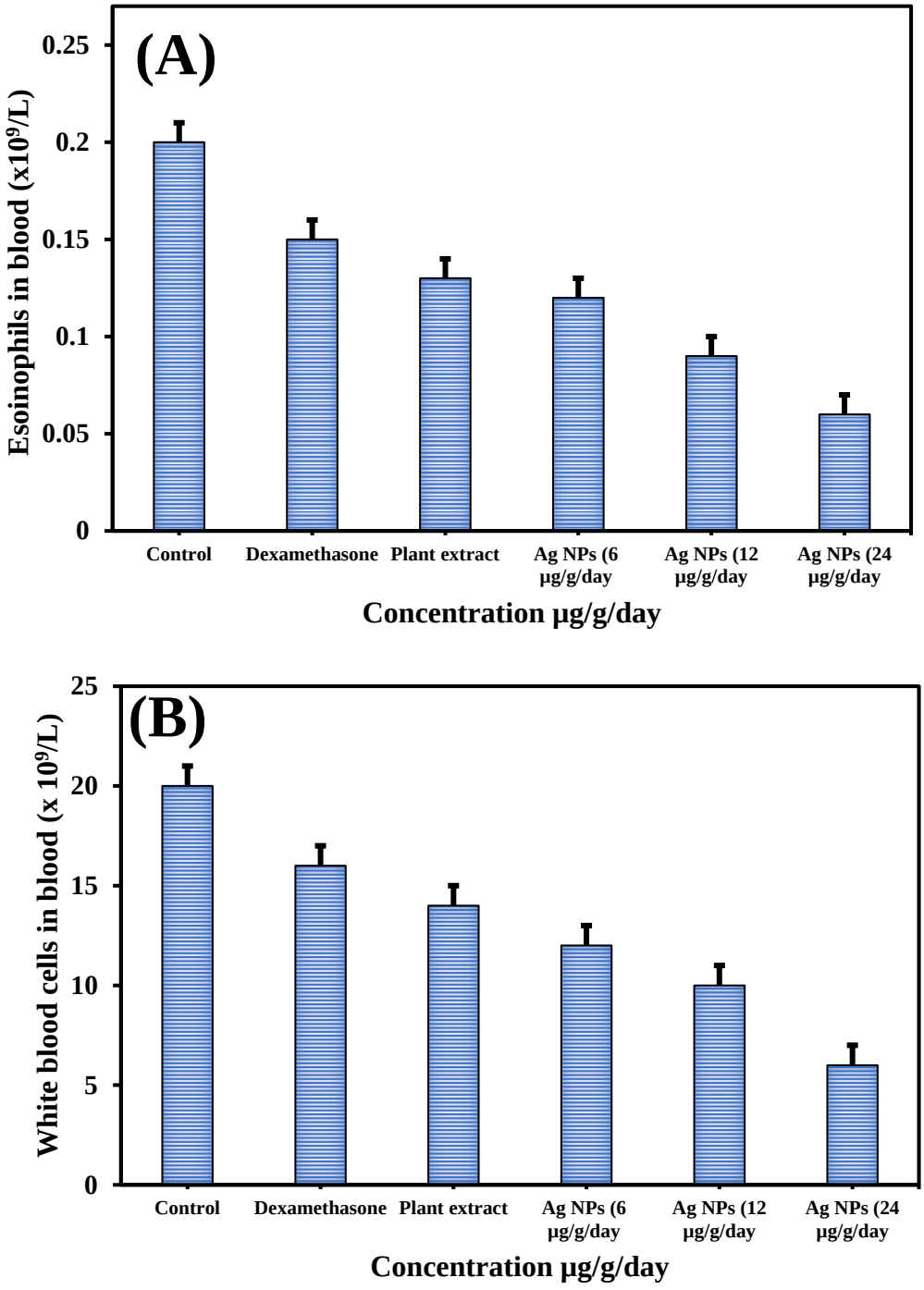

Figure 2. *Cont.*

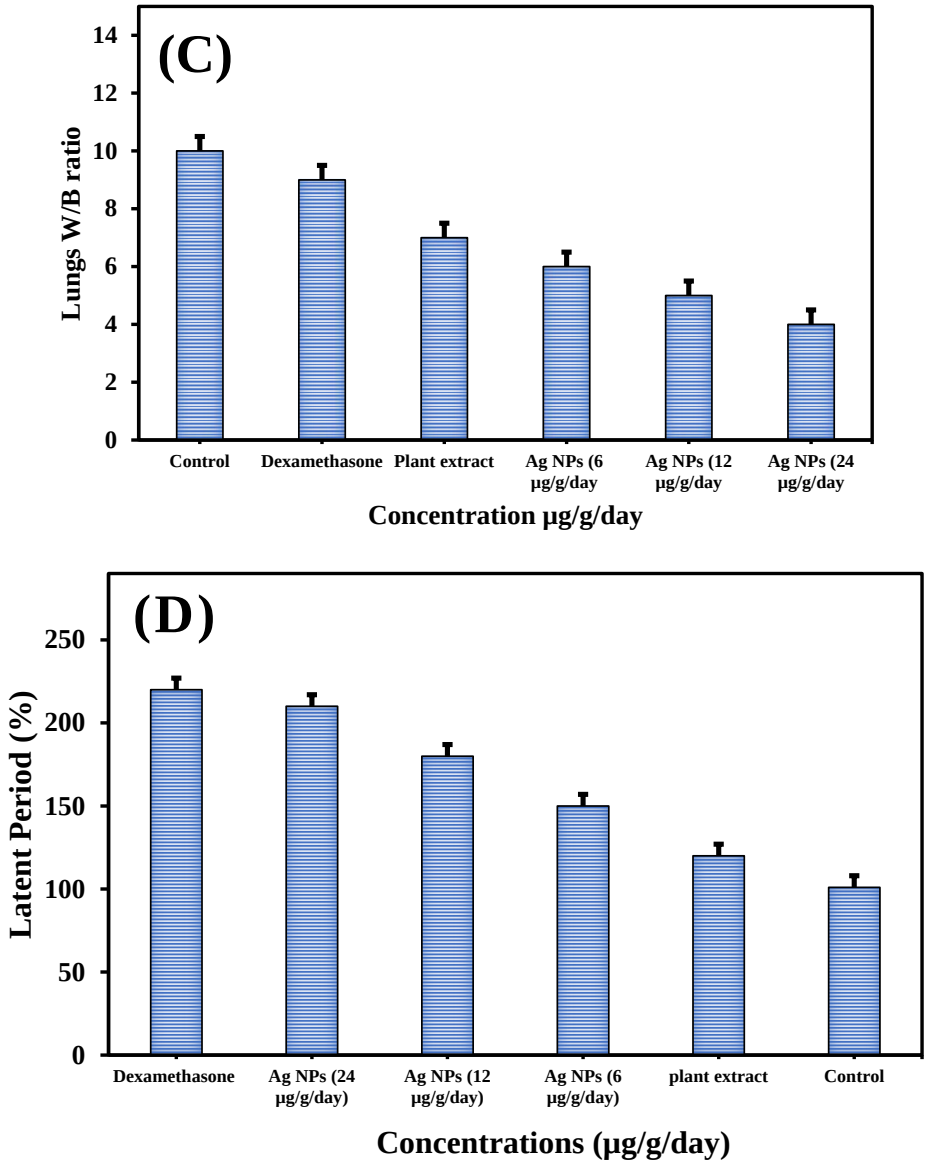

Figure 2. (**A**) Effects of the of Ag NPs on EOS Counts, (**B**) Effects of the Ag NPs on WBC Counts, (**C**) Effects of the Ag NPs on W/D Weight Ratio of Lungs (**D**) Effects of the Ag NPs on Latent Period (%).

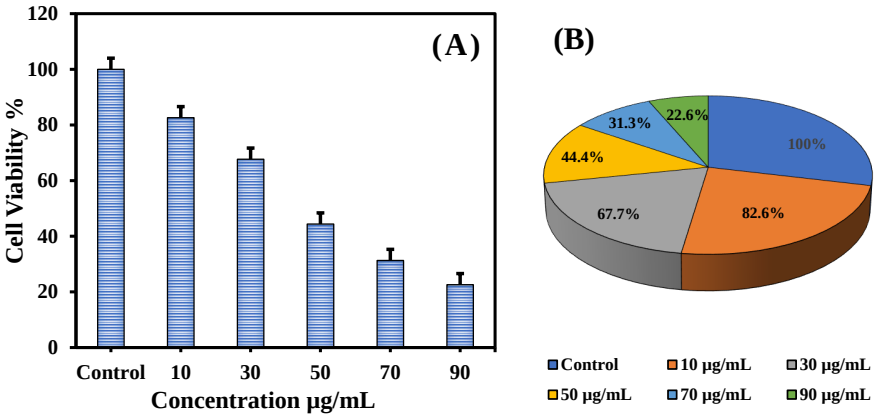

Figure 3. (**A**) Cytotoxicity of synthesized Ag NPs, (**B**) Pie chart of synthesized Ag NPs against cytotoxicity.

4. Conclusions

In the current study, an environmentally friendly, green synthesis of Ag NPs was achieved using plant extracts of *Zingiber officinale* that act as a reducing agent. The synthesis of Ag NPs was characterized by different techniques, such as UV-Visible, FT-IR, SEM, and XRD analysis. The green synthesized Ag NPs were used to evaluate the antimicrobial activity against different pathogens that showed promising activity against various bacterial and fungal strains in comparison to standard drugs. In addition, Ag NPs showed potent anti-asthma by decreasing the EOS and WBC level in the blood, the W/D ratio of lungs, and extending the latent period at concentrations of 24 µg/g/day, respectively. Furthermore, the cytotoxicity of synthesized nanoparticles tends to be at low risk in terms of their use in the industry.

Author Contributions: Conceptualization, I.A.; data curation, M.A. and N.A.; formal analysis, K.M. and F.F.; funding acquisition, F.F.; investigation, M.A.M. and K.M.; methodology, M.A.M., K.M. and F.F.; project administration, I.A.; resources, I.A.; supervision, I.A. and N.A.; validation, I.A.; writing—original draft, M.A.M., K.M. and M.A.; writing—review and editing, F.F. and I.A. All authors have read and agreed to the published version of the manuscript.

Funding: The publication charges for this article are borne from Khyber Medical University Publication Fund (No.DIR/ORIC/Ref/23/00010).

Conflicts of Interest: All the authors declare no conflict of interest.

References

1. Govindrao, J.P.; Ghule, N.W.; Bamer, A.H.; Kalaskar, M.G. Metal nanoparticles synthesis an overview on methods of preparation, advantages and disadvantages, and applications. *J. Drug Deliv. Sci. Technol.* **2019**, *53*, 101174.
2. Banerjee, P.; Satapathy, M.; Mukhopahayay, A.; Das, P. Leaf extract mediated green synthesis of silver nanoparticles from widely available Indian plants: Synthesis, characterization, antimicrobial property and toxicity analysis. *Bioresour. Bioproc.* **2014**, *1*, 3. [CrossRef]
3. Chernousova, S.; Epple, M. Silver as antibacterial agent: Ion, nanoparticle, and metal. *Angew. Chem. Int. Ed.* **2013**, *52*, 1636–1653. [CrossRef] [PubMed]
4. Amany, S.F.G.; Rab, E.; Gad, F. Effect of reducing and protecting agents on size of silver nanoparticles and their anti-bacterial activity. *Der. Pharma Chem.* **2012**, *4*, 53–65.
5. Marinescu, L.; Ficai, D.; Ficai, A.; Oprea, O.; Nicoara Vasile, B.S.; Boanta, L.; Marin, A.; Andronescu, E.; Holban, A.M. Comparative Antimicrobial Activity of Silver Nanoparticles Obtained by Wet Chemical Reduction and Solvothermal Methods. *Int. J. Mol. Sci.* **2022**, *23*, 5982. [CrossRef]
6. Skiba, M.; Vorobyova, V.; Kovalenko, I.; Shakun, A. Synthesis of Tween-Coated Silver Nanoparticles by a Plasma-Chemical Method: Catalytic and Antimicrobial Activities. *Chemistry* **2020**, *14*, 297–303. [CrossRef]
7. Krce, L.; Sprung, M.; Maravic, A.; Umek, P.; Salamon, K.; Krstulovic, N.; Aviani, I. Bacteria exposed to silver nanoparticles synthesized by laser ablation in water: Modelling, *E. coli* growth and inactivation. *Materials* **2020**, *13*, 653. [CrossRef] [PubMed]
8. Anantharaman, S.; Rego, R.; Muthakka, M.; Anties, T.; Krishna, H. Andrographis paniculata-mediated synthesis of silver nanoparticles: Antimicrobial properties and computational studies. *SN Appl. Sci.* **2020**, *2*, 1618. [CrossRef]
9. Rajagopal, T.; Jemimah, I.A.A.; Ponmanickam, P.; Ayyanar, M. Synthesis of silver nanoparticles using Catharanthus roseus root extract and its larvicidal effects. *J. Environ. Biol.* **2015**, *36*, 1283.
10. Bethu, M.S.; Netala, V.R.; Domdi, L.; Tartte, V.; Janapala, R.V. Potential anticancer activity of biogenic silver nanoparticles using leaf extract of *Rhynchosia suaveolens*: An insight into the mechanism. *Artif. Cells Nanomed. Biotechnol.* **2018**, *46*, 104–114. [CrossRef]
11. Shahrajabian, M.H.; Sun, W.; Cheng, Q. Clinical aspects and health benefits of ginger (*Zingiber officinale*) in both traditional Chinese medicine and modern industry. *Acta Agric. Scand.* **2019**, *69*, 546–556. [CrossRef]
12. Yousfi, F.; Abrigach, F.; Petrovic, J.D.; Sokovic, M.; Ramdani, M. Phytochemical screening and evaluation of the antioxidant and antibacterial potential of Zingiber officinale extracts. *S. Afr. J. Bot.* **2021**, *142*, 433–440. [CrossRef]
13. Paramita, S.; Moerad, E.B.; Ismail, S.; Marliana, E. Antiasthmatic effect of Curcuma aeruginosa extract on isolated organ of the trachea. *Research* **2018**, *7*, 1799. [CrossRef]
14. Vazquez-Munoz, R.; Meza-Villezcas, M.; Fournier, P.G.J.; Soria-Castro, E.; Juarez-Moreno, K.; Gallego-Hernandez, A.L.; Bogdanchikova, N.; Vazquez-Duhalt, R.; Saquero, H.A. Enhancement of antibiotics antimicrobial activity due to the silver nanoparticles impact on the cell membrane. *PLoS ONE* **2019**, *14*, 224904. [CrossRef]
15. Fozia, F.; Ahmad, N.; Buoharee, Z.A.; Ahmad, I.; Aslam, M.; Wahab, A.; Ullah, R.; Ahmad, S.; Alotaibi, A.; Tariq, A. Characterization and Evaluation of Antimicrobial Potential of Trigonella incise (Linn) Mediated Biosynthesized Silver Nanoparticles. *Molecules* **2022**, *27*, 4618. [CrossRef] [PubMed]

16. Gul, A.; Shaheen, A.; Ahmad, I.; Khattak, B.; Ahmad, M.; Ullah, R.; Bari, A.; Ali, S.S.; Alobaid, A.; Asmari, M.M.; et al. Green synthesis, characterization, enzyme inhibition, antimicrobial potential, and cytotoxic activity of plant mediated silver nanoparticle using *Ricinus communis* leaf and root extracts. *Biomolecules* **2021**, *11*, 206. [CrossRef]
17. Geethalakshmi, R.; Sarada, D. Synthesis of plant-mediated silver nanoparticles using Trianthema decandra extract and evaluation of their antimicrobial activities. *Int. J. Eng. Sci. Technol.* **2010**, *2*, 970–975.
18. Nakkala, J.R.; Mata, R.; Gupta, A.K.; Sadras, S.R. Biological activities of green silver nanoparticles synthesized with *Acorous calamus* rhizome extract, *Eur. J. Med. Chem.* **2014**, *85*, 784–794. [CrossRef] [PubMed]
19. Al-Radadi, N.S. *Ephedra* mediated green synthesis of gold nanoparticles (AuNPs) and evaluation of its antioxidant, antipyretic, anti-asthmatic, and antimicrobial properties. *Arab. J. Chem.* **2023**, *16*, 104353. [CrossRef]
20. Mei, F.; Xing, X.F.; Tang, Q.F.; Chen, F.L.; Guo, Y.; Song, S.; Tan, X.M.; Luo, J.B. Antipyretic and anti-asthmatic activities of traditional Chinese herb-pairs, Ephedra and Gypsum. *Chin. J. Integr. Med.* **2016**, *22*, 445–450. [CrossRef]
21. Kim, H.J.; Lee, H.J.; Jeong, S.J.; Lee, H.J.; Kim, S.H.; Park, E.J. Cortex Mori Radicis extract exerts antiasthmatic effects via enhancement of CD^{4+} CD^{25+} $Foxp^{3+}$ regulatory T cells and inhibition of Th2 cytokines in a mouse asthma model. *J. Ethnopharmacol.* **2011**, *138*, 40–46. [CrossRef] [PubMed]
22. Sakai-Kashiwabara, M.; Asano, K. Inhibitory action of quercetin on eosinophil activation in vitro. *Evid. -Based Complement. Altern. Med.* **2013**, *2013*, 127105. [CrossRef] [PubMed]
23. Chu, S.J.; Huang, K.L.; Wu, S.Y.; Ko, F.C.; Wu, G.C.; Li, R.Y.; Li, M.H. Systemic administration of FC-77 dampens ischemia–reperfusion-induced acute lung injury in rats. *Inflammation* **2013**, *36*, 1383–1392. [CrossRef] [PubMed]
24. Qasim, M.; Nasar, T.; Zohra Khalil, A.T.; Saqib, S.; Ayaz, M.; Ahmad, A.; Shinwari, Z.K. *Seripheidium quettense* mediated green synthesis of biogenic silver nanoparticles and their theranostic applications. *Green Chem. Lett. Rev.* **2019**, *12*, 310–322. [CrossRef]
25. Awwad, A.M.; Salem, N.M. Green synthesis of silver nanoparticles by Mulberry Leaves Extract. *Nanosci. Nanotechnol.* **2012**, *2*, 125–128. [CrossRef]
26. Bhakya, S.; Muthukrishnan, S.; Sukumaran, M.; Muthukumar, M. Biogenic synthesis of silver nanoparticles and their antioxidant and antibacterial activity. *Appl. Nanosci.* **2016**, *6*, 755–766. [CrossRef]
27. Mason, C.; Vivekanandhan, S.; Misra, M.; Mohanty, A.K. Switchgrass (*Panicum virgatum*) extract mediated green synthesis of silver nanoparticles. *World J. Nano Sci. Eng.* **2012**, *2*, 47. [CrossRef]
28. Varghese, B.; Kurian, M.; Krishna, S.; Athira, T.S. Biochemical synthesis of copper nanoparticles using *Zingiber officinalis* and *Curcuma longa*: Characterization and antibacterial activity study. *Mater. Today Proc.* **2020**, *25*, 302–306. [CrossRef]
29. Wang, C.; Kim, Y.J.; Singh, P.; Mathiyalagan, R.; Jin, Y.; Yang, D.C. Green synthesis of silver nanoparticles by *Bacillus methylotrophic* us, and their antimicrobial activity. *Artif. Cells Nanomed. Biotechnol.* **2016**, *44*, 1127–1132.
30. Ghasemzadeh, A.; Jaafar, H.Z.; Rahmat, A. Antioxidant activities, total phenolics and flavonoids content in two varieties of Malaysia young ginger (*Zingiber officinale* Roscoe). *Molecules* **2010**, *15*, 4324–4333. [CrossRef] [PubMed]
31. Shaikh, W.A.; Chakraborty, S.; Owens, G.; Islam, R.U. A review of the phytochemical mediated synthesis of Ag NP (silver nanoparticle): The wonder particle of the past decade. *Appl. Nanosci.* **2021**, *11*, 2625–2660. [CrossRef] [PubMed]
32. Albukhari, S.M.; Ismail, M.; Akhtar, K.; Danish, E.Y. Catalytic reduction of nitrophenols and dyes using silver nanoparticles cellulose polymer paper for the resolution of waste water treatment challenges. *Colloids Surf. A Physicochem. Eng. Asp.* **2019**, *577*, 548–561. [CrossRef]
33. Aziz, B.; Hussein, S.; Brza, G.; Mohammed, M.A.J.; Abdulwahid, S.T.; Raza Saeed, R.; Hassanzadeh, A. Fabrication of interconnected plasmonic spherical silver nanoparticles with enhanced localized surface plasmon resonance (LSPR) peaks using quince leaf extract solution. *Nanomaterials* **2019**, *9*, 1557. [CrossRef]
34. Kim, H.S.; Seo, Y.S.; Kim, K.; Han, J.W.; Park, Y.; Cho, S. Concentration effect of reducing agents on green synthesis of gold nanoparticles: Size, morphology, and growth mechanism. *Nanoscale Res. Lett.* **2016**, *11*, 1–9. [CrossRef]
35. Sganzerla, W.G.; Longo, M.; de Oliveira, J.L.; da Rosa, C.G.; de Lima Veeck, A.P.; de Aquino, R.S.; Masiero, A.V.; Bertoldi, F.C.; Barreto, P.L.M.; Nunes, M.R. Nanocomposite poly (ethylene oxide) films functionalized with silver nanoparticles synthesized with Acca sellowiana extracts. *Colloids Surf. A Physicochem. Eng. Asp.* **2020**, *602*, 125125. [CrossRef]
36. Johnson, P.; Krishnan, V.; Loganathan, C.; Govindhan, K.; Raji, V.; Sakayanathan, P.; Sathishkumar, P.; Palvannan, T. Rapid Biosynthesis of *Bauhinia variegata* Flower Extract-Mediated Silver Nanoparticles: An Effective Antioxidant Scavenger and α-Amylase Inhibitor. *Artif. Cells. Nanomed. Biotechnol.* **2018**, *46*, 1488–1494. [CrossRef]
37. Jena, J.; Pradhan, N.; Dash, B.P.; Sukla, L.B.; Panda, P.K. Biosynthesis and characterization of silver nanoparticles using microalga *Chlorococcum humicola* and its antibacterial activity. *Int. J. Nanomater. Biostruct.* **2013**, *3*, 1–8.
38. Prabu, H.J.; Johnson, I. Plant-mediated biosynthesis and characterization of silver nanoparticles by leaf extracts of *Tragia involucrata*, *Cymbopogon citronella*, *Solanum verbascifolium* and *Tylophora ovata*. *Karbala Int. J. Mol. Sci.* **2015**, *1*, 237–246. [CrossRef]
39. Raut, R.W.; Mendhulkar, V.D.; Kashid, S.B. Photosensitized synthesis of silver nanoparticles using *Withania somnifera* leaf powder and silver nitrate. *J. Photochem. Photobiol. B Biol.* **2014**, *132*, 45–55. [CrossRef]
40. Feng, Q.L.; Wu, J.; Chen, G.; Cui, F.; Kim, T.; Kim, J. A mechanistic study of the antibacterial effect of silver ions on *Escherichia coli* and *Staphylococcus aureus*. *J. Biomed. Mater. Res.* **2000**, *52*, 662–668. [CrossRef]
41. Periasamy, S.; Jegadeesan, U.; Sundaramoorthi, K.; Rajeswari, T.; Tokala, V.N.B.; Bhattacharya, S.; Muthusamy, S.; Sankoh, M.; Nellore, M.K. Comparative Analysis of Synthesis and Characterization of Silver Nanoparticles Extracted Using Leaf, Flower, and Bark of *Hibiscus rosasinensis* and Examine Its Antimicrobicidal Activity. *J. Nanomater.* **2022**, *2022*, 8123854. [CrossRef]

42. Abboud, Y.; Saffaj, T.; Chagraoui, A.; El Bouari, A.; Brouzi, K.; Tanane, O.; Ihssane, B. Biosynthesis, characterization and antimicrobial activity of copper oxide nanoparticles (CONPs) produced using brown alga extract (*Bifurcaria bifurcata*). *Appl. Nanosci.* **2014**, *4*, 571–576. [CrossRef]
43. Sridhara, V.; Prathima, K. Vegetable assisted synthesis of silver nanoparticles and its antibacterial activity against two human pathogens, *Asian. J. Pharm. Clin. Res.* **2013**, *6*, 974–2441.
44. Panacek, A.; Kolar, M.; Vecerova, R.; Prucek, R.; Soukupova, J.; Krystof, V.; Hamal, P.; Zboril, R.; Kvitek, L. Antifungal activity of silver nanoparticles against *Candida* spp. *Biomaterials* **2009**, *30*, 6333–6340. [CrossRef] [PubMed]
45. Pallavi, S.S.; Rudayni, H.A.; Bepari, A.; Niazi, S.K.; Nayaka, S. Green synthesis of Silver nanoparticles using *Streptomyces hirsutus* strain SNPGA-8 and their characterization, antimicrobial activity, and anticancer activity against human lung carcinoma cell line A549. *Saudi J. Biol. Sci.* **2022**, *29*, 228–238.
46. Singh, A.; Dar, M.Y.; Joshi, B.; Sharma, B.; Shrivastava, S.; Shukla, S. Photofabrication of silver nanoparticles: Novel drug to overcome hepatocellular ailments. *Toxicol. Rep.* **2019**, *5*, 333–342. [CrossRef] [PubMed]
47. Li, G.; Liu, L.; Sun, Y.; Liu, L. Ecofriendly synthesis of silver–carboxy methyl cellulose nanocomposites and their antibacterial activity. *J. Clus. Sci.* **2018**, *29*, 1193–1199. [CrossRef]
48. Nasar, M.Q.; Khalil, A.T.; Ali, M.; Shah, M.; Ayaz, M.; Shinwari, Z.K. Phytochemical analysis, *Ephedra Procera* CA Mey. Mediated green synthesis of silver nanoparticles, their cytotoxic and antimicrobial potentials. *Medicine* **2019**, *55*, 369.
49. Ovais, M.; Khalil, A.T.; Raza, A.; Khan, M.A.; Ahmad, I.; Islam, N.U.; Saravanan, M.; Ubaid, M.F.; Ali, M.; Shinwari, Z.K. Green synthesis of silver nanoparticles via plant extracts: Beginning a new era in cancer theranostics. *Nanomedicine* **2016**, *12*, 157–3177. [CrossRef]